Title

An Inhibitor of GSK3B and HDACs Kills Pancreatic Cancer Cells and Slows Pancreatic Tumor Growth and Metastasis in Mice

Journal

Gastroenterology, 155(6)

ISSN

0016-5085

Authors

Edderkaoui, Mouad
Chheda, Chintan
Soufi, Badr
et al.

Publication Date

2018-12-01

DOI

10.1053/j.gastro.2018.08.028

Peer reviewed

HHS Public Access

Author manuscript

Gastroenterology. Author manuscript; available in PMC 2019 December 01.

Published in final edited form as:

Gastroenterology. 2018 December ; 155(6): 1985–1998.e5. doi:10.1053/j.gastro.2018.08.028.

An Inhibitor of GSK3B and HDACs Kills Pancreatic Cancer Cells and Slows Pancreatic Tumor Growth and Metastasis in Mice

Mouad Edderkaoui[1,2], **Chintan Chheda**[1], **Badr Soufi**[1], **Fouzia Zayou**[1], **Robert W. Hu**[1], **V. Krishnan Ramanujan**[1], **Xinlei Pan**[1], **Laszlo G. Boros**[2], **Jian Tajbakhsh**[1], **Anisha Madhav**[1], **Neil A. Bhowmick**[1], **Qiang Wang**[1], **Michael Lewis**[3], **Richard Tuli**[1], **Aida Habtezion**[4], **Ramachandran Murali**[1], and **Stephen J. Pandol**[1,2]

[1]Departments of Medicine, Biomedical Sciences, Radiation Oncology and Surgery, Samuel Oschin Comprehensive Cancer Center, Cedars-Sinai Medical Center, Los Angeles, California

[2]Department of Pediatrics, University of California at Los Angeles, California

[3]Veterans Affairs, West Los Angeles, CA

[4]Division of Gastroenterology and Hepatology, Department of Medicine, Stanford University School of Medicine, Stanford, CA.

Abstract

Background & Aims: Growth, progression, and drug resistance of pancreatic ductal adenocarcinomas (PDACs) have been associated with increased levels and activity of glycogen synthase kinase 3 beta (GSK3B) and histone deacetylases (HCACs). We designed and synthesized molecules that simultaneously inhibit the activities of both enzymes. We tested the effects of one of these molecules, metavert, in pancreatic cancer cells and mice with pancreatic tumors.

Methods: We tested the ability of metavert to bind GSK3B and HDACs using surface plasmon resonance. MIA PaCa-2, Bx-PC3, HPAF-II, and HPDE6 cell lines were incubated with different concentrations of metavert, with or without paclitaxel or gemcitabine, or with other inhibitors of GSK3B and HDACs; cells were analyzed for apoptosis and migration and by immunoblotting,

Correspondence: Mouad Edderkaoui, PhD, 8700 Beverly Boulevard, Davis 3100, Los Angeles, CA 90048. Tel: 310-248-8024; mouad.edderkaoui@cshs.org.

Authors contributions:
Edderkaoui: Study concept and design, data acquisition and analysis, and manuscript drafting. Chheda, Soufi, Zayou, Hu, Wang: Acquisition of data.
Lewis: Analyzing tissue.
Habtezion: Multiplexing data.
Ramanujan and Boros: Metabolic studies.
Madhav and Bhowmick: Developing the UN-KPC961-Luc cells.
Murali, Pan: Design of the structure of the drug and SPR studies.
Tuli: Irradiation data.
Tajbakhsh: Nuclear localization assays.
Pandol: Study concept and design and contribution in drafting manuscript.

Disclosure of conflict of interest: The authors Edderkaoui, Murali, Habtezion and Pandol disclose their relationship with Avenzoar Pharmaceuticals. Edderkaoui, Murali and Pandol are co-inventors in the patent related to metavert. Other authors have no conflict of interest.

immunofluorescence, and real-time PCR. Krasþ/LSLG12D;Trp53þ/LSLR172H;Pdx-1-Cre (KPC) mice (2 months old) were given injections of metavert (5 mg/Kg, 3 times/week) or vehicle (control). B6.129J mice with tumors grown from UN-KPC961-Luc cells were given injections of metavert or vehicle. Tumors and metastases were counted and pancreata were analyzed by immunohistochemistry. Glucose metabolism was measured using 13C-glucose tracer and mass spectroscopy and flow cytometry. Cytokine levels in blood samples were measured using multiplexing ELISA.

Results: Metavert significantly reduced survival of PDAC cells but not non-transformed cells; the agent reduced markers of the epithelial to mesenchymal transition and stem cells in PDAC cell lines. Cells incubated with metavert in combination with irradiation and paclitaxel or gemcitabine had reduced survival compared to cells incubated with either agent alone; metavert increased killing of drug-resistant PDAC cells by paclitaxel and gemcitabine. PDAC cells incubated with metavert acquired normalized glucose metabolism. Administration of metavert (alone or in combination with gemcitibine) to KPC mice or mice with syngeneic tumors significantly increased their survival times, slowed tumor growth, prevented tumor metastasis, decreased tumor infiltration by tumor-associated macrophages, and decreased blood levels of cytokines.

Conclusions: In studies of PDAC cells and 2 mouse models of PDAC, we found a dual inhibitor of GSK3B and HDACS (metavert) to induce cancer cell apoptosis, reduce migration and expression of stem cell markers, and slow growth of tumors and metastases. Metavert had synergistic effects with gemcitabine.

Keywords

Pancreas; neoplasm; EMT; chemotherapeutic agent

INTRODUCTION:

PDAC (aka pancreatic cancer) is a disease with no effective treatment and with one of the lowest survival rates of any cancer. One of the major reasons for such a poor outcome is the simultaneous activation of multiple pro-cancer pathways in the cancer cells which allows them to overcome treatments based on the inhibition of a single oncogenic pathway.

In most patients with PDAC chemotherapy and radiation are the current standard treatments that include Gemcitabine, Abraxane and the FOLFIRINOX combination regimen. Each of these treatments shows significant toxicity and marginal durable efficacy. One of the reasons for their poor efficacy is that the treatments themselves stimulate pro-cancer pathways leading to induction of their resistance to death[1]. How these treatments lead to resistance remains unknown. Nonetheless, none of the current treatments used have been successful in affecting pathways leading to drug resistance and metastasis.

It is increasingly recognized that drugs targeting multiple tumor-survival pathways provide an advantage over single targeted therapy. For example, pan-protein tyrosine kinase inhibitor drugs such as Sorafinib and Lapatinib, have been used in the treatment of advanced kidney, liver and breast cancers[2]. However, similar drugs that can target multiple pathways have not been identified for PDAC treatment.

Post-translational and epigenetics changes are widely involved in cancer development[3]. In this regard, Glycogen synthase kinase-3 beta (GSK3B) is an ubiquitously expressed serine/threonine kinase involved in metabolism, oncogenesis and neurological diseases that plays a role in PDAC[4]. GSK3B up-regulates NF-κB activity that stimulates pathways involved in cell proliferation, production of pro-tumorigenic cytokines and development of resistance to apoptosis in PDAC cells[5, 6] In a study using orthotopic model of PDAC, a GSK3B inhibitor caused inhibition of NF-κB activity and shrinkage of tumors[7]. Unexpectedly, GSK3B inhibition enhanced transcription factors that promote epithelial to mesenchymal transition (EMT) such as Snail.[8, 9]. EMT pathways are responsible for tumor invasion and metastasis[10, 11]. The EMT transcription factor Zeb1 expression is associated with the mesenchymal phenotype in PDAC cells[12, 13] and inhibition of GSK3B induces EMT[14, 15]. These results suggest that GSK3B simultaneously plays two roles: **(1)** Pro-cancer role by inducing NF-κB activation; **(2)** anti-cancer role by preventing EMT and metastasis. Thus, a strategy to inhibit GSK3B alone poses a conundrum.

The transcription factor Zeb1, activated by GSK3B, mediates EMT by stabilizing histone deacetylase-1 (HDAC1) in PDAC cells[12]. We have shown that the pan-HDAC class I and II inhibitor Saha limited pancreatic lesion formation in a PDAC Pdx-Cre;LSL-Kras (KC) mice[16,17]. With this background, we hypothesized that co-targeting GSK3B and HDAC would not only increase killing of the cancer and prevent their resistance to apoptosis, but would also inhibit pro-EMT/metastasis and drug resistance.

Towards this goal, here, we describe the design, synthesis and testing of a novel dual inhibitor, called metavert (a trademark owned by Avenzoar Pharmaceuticals), on PDAC cell survival, migration, cancer stemness and glucose metabolism. We further tested metavert in one of the most aggressive animal models of advanced PDAC using the KPC mice[18] as well as in a syngeneic mouse model of PDAC. Our studies show that metavert increased the survival of mice in both models and prevented metastasis by affecting both tumor cells' proliferation, metabolic profiles, and different markers of advanced cancer without affecting healthy organs.

METHODS:

Chemicals:

Metavert was synthesized by AMRI (Albany Molecular Research Institute, Albany, NY). Saha was purchased from Cayman (Ann Arbor, MI). Alpha-smooth muscle actin (αSMA) antibody was purchased from Sigma-Aldrich (St. Louis, MO); Sirius Red/Collagen Staining Kit was from Chondrex (Redmond, WA); F4/80, PE/Cy7-CD44, FITC-CD24 and vimentin antibodies from AbCam (Cambridge, MA); Arginase1 from Santa Cruz Biotechnology (Santa Cruz, CA); other antibodies were from Cell signaling (Danvers, MA). All other chemicals were from Sigma Aldrich (St. Louis, MO).

Cell culture experiments:

Poorly differentiated MIA PaCa-2, moderately differentiated Bx-PC3, and moderately to well differentiated HPAF-II human PDAC cell lines were obtained from the American Type

Culture Collection (Manassas, VA). MIA PaCa-2 cells were grown in 1/1 D-MEM/F-12 medium supplemented with 15% fetal bovine serum (FBS), 4 mM L-glutamine, and 1% of antibiotic/antimycotics solution. Bx-PC3 and HPAF-II were grown in RPMI-1640 supplemented with 10% fetal bovine serum (FBS) and 1% of antibiotic/antimycotics solution. The immortalized human pancreatic duct epithelial cell line, HPDE6-c7, was a gift from Dr. M-S Tao (Ontario, Canada)[19, 20]. The HPDE6-c7 cells were grown in keratinocyte serum free (KSF) medium supplemented with bovine pituitary extract (25 μg/500 ml), epidermal growth factor (2.5 μg/500 ml), penicillin (100 U/ml), and streptomycin (100 μg/ml). Cells were maintained at 37°C in a humidified atmosphere containing 5% CO_2 and were used between passages 2 and 10. Gemcitabine-resistant MIA PaCa-2 cells were generated by culturing MIA PaCa-2 cells in increasing doses gemcitabine (1, 5, 30, 60 and 120 ng/ml) for 2-3 weeks in each dose.

Cell survival and migration measurements:

Survival was measured by MTT assay[21]. Apoptosis was measured using Cell Death Detection ELISA^{Plus} kit (Roche Molecular Biochemicals, Manheim, Germany)[22-24]. Migration was assessed by using the Matrigel Invasion Chamber Assay (Corning, Bedford, MA).

Glucose metabolic pathways measurement:

Glucose uptake and superoxide levels in live cells were measured by flow cytometry analysis by labeling with 2NBDG (50μM) and MitoSox Red (2.5 μM) (Life Technologies, Grand Island, NY). Lactate measurements and mitochondrial respiration measurements were carried out as described earlier[25, 26]. 13C-Glucose tracer and mass spectroscopy analysis was used as shown before[27].

Animals:

All animal studies are performed according to the guidence of IACUC and afer the approval of IACUC (Protocol # 3688), Cedars-Sinai Medical Center. We used the KPC mouse model of PDAC developed by Hingorani et al.[18]. Mice were intraperitoneally injected starting from the age of 2 months 3 times per week with 5mg/Kg of metavert or vehicle (14 KPC mice per group). Metavert was dissolved in a mixture of 50% N, N-dimethylacetamide (DMA), 45% polyethylene glycol 400 (PEG-400) and 5% Tween-80 (solution A). Before injections, dissolved metavert was diluted 3 times in saline and injected intraperitoneally. Control mice were injected with Solution A diluted 3 times in saline. Mice were injected 3 times per week until death occurred or mice were ordered by veterinarian to be euthanized. Mice were intraperitoneally injected weekly with 10mg/Kg of Gemcitabine alone or with injections of metavert.

In a different set of mice, we injected KPC mice with metavert or control solution (6 KPC mice per group) starting from age of 2 months and sacrificed them at 4 months of age.

Syngeneic mouse model of PDAC:

5 10^5 UN-KPC961-Luc cells were injected into the pancreas of B6.129J (2 months old). Mice were separated in two sets. Set 1 (6 mice per group) received vehicle or metavert

(5mg/Kg) ip injections 3 times per week until death or sacrificed when reaching the age of 4 months old. In set 2 (4 mice per group), mice were treated like in set 1 but sacrificed after 4 weeks of treatment to compare tissues.

Survival of treated mice versus control mice:

All mice were monitored at least three times weekly. For survival studies, mice were injected by a blinded person and followed until death or euthanized by a blinded observer when signs of morbidity were evident. Euthanasia was ordered if there was a weight loss of at least 20% or in the condition of a complete anorexia for 24 hours or partial anorexia for 3 days accompanied with weakness and inability to move and to obtain food and/or water.

Tissue immunostaining and Western blot analysis were performed as before[28].

Immunofluorescence assay and confocal imaging and analysis of cultured cells:

Cells were fixed with 4% paraformaldehyde/phosphate buffered saline, and permeabilized using 0.5% Saponin/0.5% triton X-100 and blocked with 3% bovine serum albumin (Roche), prior to indirect immunofluorescence labeling. Unconjugated primary antibodies used were: monoclonal mouse anti-GSK3B (Antibody Plus, Cat. # STJ98120) at 1:500 dilution, and monoclonal rabbit anti-H3K9Ac (Cell Signaling Technology, Cat. #9646) at 1:400 dilution. Confocal imaging of labeled cells was performed using a TCS SP5 X supercontinuum microscope (Leica Microsystems)[29, 30].

Luminex assays:

Luminex assay was performed at Stanford Human Immune Monitoring Center as recommended by the manufacturer (Panomics/Affymetrix)[31].

Binding study:

Binding analysis of HDAC2 and metavert was performed using SBGIRD software[32]. The X-ray crystal structure coordinates for human HDAC2 in complex with Saha (PDB 4LXZ)[33] was retrieved from the RCSB Protein Data Bank (PDB) and prepared with the Protein Preparation Wizard in MAESTRO v9.2 (Schrodinger, Inc. San Diego, CA). The optimized protein structure was then subjected to all-atom constrained energy minimization using the IMPREF module of MAESTRO v9.2 with OPLS-2005 force field (Schrodinger, Inc.). The prepared HDAC2 structure was used for the molecular docking simulations. The prepared Saha and metavert molecules were docked flexibly utilizing GLIDE v5.7 standard precision (SP) and GLIDE extra precision (XP) scoring functions[34] using standard protocols. The best docking positions were selected based on the total binding energy and the number of contacts.

Liver and kidney injury measurements:

Measurement of the serum were performed according to the protocols in their respective kits (Biomedical Research Service Center, University at Buffalo, State University of New York, NY).

Statistics:

Statistical analyses were performed by using Student's t test, one-way ANOVA, or Fisher's exact test with GraphPad Prism (GraphPad Software). The log-rank (Mantel-Cox) test was used to analyze survival data. A p value < 0.05 was considered statistically significant.

RESULTS:

Inhibiting both GSK3B and HDAC decreased cell survival and markers of EMT greater than blocking either GSK3B or HDAC in pancreatic cancer cells:

GSK3B and multiple HDACs have been shown to be highly expressed in human PDAC[7, 35, 36]. In mice, expression of GSK3B is high in PDAC tissue compared to normal tissue (Fig. S1A). At least two HDACs including HDAC4 and HDAC7 as well as the phosphorylated form of HDAC7 are highly present in pancreatic tumor tissues of KPC mice compared to pancreatic normal tissues from mice of the same background (Fig. S1B).

To test the hypothesis that blocking both GSK3B and HDAC-I/II will be more effective than inhibition of either pathway individually, we used Saha (HDAC-I/II inhibitor) and Tideglusib (GSK3B inhibitor) which are currently FDA approved or in clinical trials [37, 38]. The combination of small doses of Saha and tideglusib induced an additive decrease in cancer cell survival (Fig. S1C) in PDAC cells. Treatment with Tideglusib alone resulted in an increase of EMT marker vimentin but not Twist and Snail. However, treatment with Saha alone or in combination with Tideglusib induced a decrease in the protein level of all EMT markers (Fig. S1D). Similarly, GSK3B siRNA induced increase in EMT markers and this effect was prevented by HDAC I/II inhibition (Fig. S1E). Therefore, the combination of Saha and Tideglusib has an additive effect on preventing cancer cell survival and promoting a decrease in markers of EMT. However, it is widely recognized that multiple-drug combination treatment is inferior to multi-targeted single drugs due to variation in their PK/PD and potential drug-drug interaction[39]. To overcome this issue, we designed and developed a novel dual agent to disable both GSK3B and HDAC functions. We targeted the classes I and II of HDAC because previously published data showed their involvement in PDAC progression[28].

Design and development of metavert and its effects *in vitro:*

The three-dimensional structures of Saha and Tideglusib bounds to their respective targets are available[40, 41]. Based on the chemical structures of Saha and Tideglusib (TDZD) we designed the novel molecule, metavert, which contains active pharmacophores to bind to both GSK3B and HDAC (classes I and II). Briefly, pharmacophores from the crystal structures of HDAC and GSK3B were derived. Using a geometrical constrain approach, series of linkers were designed and multiple analogs were synthesized. Synthesis of metavert and its analogs was performed by the Albany Molecular Research Institute (AMRI, Albany, NY).

The structure of metavert is shown in the figure 1A. To validate that metavert can mimic HDAC inhibitor and bind to HDAC, we used computer based modeling and surface plasmon resonance. Of note, the exact binding site for Tideglusib is not known; it has been reported

to be a non-ATP competitive binder[42]. Hence, binding mode of metavert to GSK3B could not be assessed. The results showed that metavert mimics the binding mode of Saha, a pan-inhibitor of HDAC class of proteins (Fig. 1B) but its affinity is weaker based on the binding energy of metavert and Saha.

To demonstrate that metavert physically interacts with its targets, HDAC and GSK3B, we performed binding analysis using surface plasmon resonance (SPR) as described in Park et. *al*.[43]. Analysis showed that metavert binds to both recombinant HDAC2 and GSK3B (Fig. 1C-D) with an affinity of 12.8 μM and 1μM, respectively.

Figure S2A shows the synthesis steps of metavert. In addition to metavert, two analogs showed a significant anti-survival effect in cancer cells. The structures of the two molecules (CSME-188543 and CSME-185643) are shown (Fig. S2B-C). Significance of the anti-survival effect of both analogs was achieved in the low 100 nano-molar range (Fig. S2D).

Next, in a cell based screen for its biological activity, metavert dose-dependently decreased cell survival of PDAC cell lines BxPC3, MIA PaCa-2 and HPAF-II and had no effect on the cell survival of human non-cancer pancreatic ductal HPDE6 cells (Fig. 2A). HPAF-II was more sensitive to metavert than BxPC-3 and MIA PaCa-2 cells. Furthermore, metavert showed a more potent effect on killing cancer cells when compared to the combination of two independent inhibitors of HDAC-I/II and GSK3B (Fig. 2B). More importantly, combination of metavert with standard treatments such as low-dose of irradiation (4Gy), paclitaxel or gemcitabine reduced cell survival by a level greater than the combination of the effects separately indicating a synergistic anti-cancer effect (Fig. 2C-E). More importantly, we developed a gemcitabine-resistant clone of MIA PaCa-2 cells and tested both gemcitabine and metavert on survival of these cells. We found that metavert re-sensitized the resistant cells to gemcitabine (Fig. 2F).

EMT is the driving force of migration of the cancer cells through up regulation of transcription factors, N-cadherin and Twist. We found that metavert decreased the level of markers of EMT such as N-cadherin and Twist as shown by Western analysis (Fig. 3A). The decrease in the protein level of N-cadherin and Twist were found at very low doses (150nM). Furthermore, metavert decreased migration of MIA PaCa-2 cells at a low dose of 150nM by 40% and completely inhibited cell migration at 600nM (Fig. 3B).

EMT is usually associated with cancer stemness, the main driving force of resistance to treatments. Therefore, we analyzed the effect of metavert on cancer stemness markers. Metavert decreased the mRNA level of various markers such as Sox2, CD133, and Nanog (Fig. 3C). Importantly, we found that the anti-PDAC chemotherapy drug Abraxane increased the level of cancer stemness marker CD44. This increase was prevented when combining Abraxane with metavert (Fig. 3D) suggesting that metavert will not only increase the cancer cell killing effect of chemotherapies as shown earlier, but will also prevent resistance that develops with other chemotherapeutic agents.

Finally, it’s worth noting that metavert affected the canonical pathways as shown by an increase in histone acetylation and phosphorylation/inhibition of GSK3B (serine 9) by Western (Fig. 4A). Next, we co-immunolabeled GSK3B and H3K9 acetylation (H3K9Ac) in

MIA PaCa-2 cancer cells and quantified fluorescent intensity in the nucleus. Maximum intensity projections of confocal images of cells showed increase in H3K9Ac in the nuclei of metavert-treated cells (Fig. 4B). Quantitative results of cell-by cell high-content analysis prove that metavert induced a 62% greater abundance of H3K9Ac, and in conjunction, an increase in H3K9Ac/DAPI co-localization (indicated by the angle of the co-localization slope: δ=4.2° versus δ=22.7°) on average across exposed cells (Fig. 4C-a, b). Representative scatter plots of individual cells indicate that H3K9Ac/DAPI co-localization slope was significantly increased by metavert (Fig. 4C-d). In contrast, quantitative results of high-content analysis show no significant change in nuclear GSK3B content and nuclear co-distribution with DAPI (δ=2.3° versus δ=4.1°) (Fig. 4C-a, b), as confirmed by scatter plots of single representative cells (4C-c). In summary, we report an increase in H3K9Ac in the nucleus of cells treated with metavert with no change in the level and distribution of GSK3B; although GSK3B phosphorylation of serine 9 inducing its inhibition was increased by metavert.

Metavert improves overall survival and prevents metastasis in advanced pancreatic cancer mouse models:

One of the distinct features of PDAC is the short survival time after diagnosis. While there are many factors that determine when the cancer is manifested, metastasis is often found at the time of diagnosis. To test whether metavert can prevent advanced PDAC and metastasis, we used an aggressive transgenic mouse model of PDAC using the KPC mice[18]. We treated KPC mice starting from the age of 2 months with intraperitoneal injections of metavert (5mg/Kg) 3 times per week. We chose this time point because, from our previous experience with these mice, 100% of the KPC mice have already developed cancer at this age. KPC mice start developing cancer lesions from the age of 4-6 weeks[18]. The treatment was pursued until natural death of a mouse occurred or euthanasia ordered by a blinded veterinarian (Fig. 5A). Euthanasia was ordered if there was a weight loss of at least 20% or in the condition of a complete anorexia for 24 hours or partial anorexia for 3 days accompanied with weakness and inability to move and to obtain food and/or water.

Metavert significantly improved the survival of KPC mice compared to control-treated KPC mice. When 57% of control mice died 100% of metavert-treated mice were still alive; and when all control mice were dead 42% of metavert-treated mice were still alive. The median survival time of mice significantly increased from 120 days in control treated mice to 173 days in metavert-treated mice (Fig. 5B).

The average tumor weight at the time of death was decreased by metavert by 50% (Fig. 5C). More importantly, we found no visible metastasis in the liver or lung of the metavert-treated mice compared to visible metastasis in 29% of control mice (Fig. 5D). Histological analysis of the pancreatic mouse tissues showed presence of cancer with a desmoplastic reaction and absence of normal-looking tissue in the pancreas of control mice; whereas, metavert-treated mice had cancer with desmoplastic reaction with presence of some normal-looking acinar cells (Fig. 5E). CK19 staining showed the presence of a diffuse cytoplasmic staining in tumor cells in the pancreas and in metastatic cancer cells in the liver. The staining shows absence of cancer cells in the liver of Metavert-treated mice (Fig. 5F)[44] The metastasis data

was further confirmed by performing a S100P staining showing presence of metastases in control liver tissues and absence of metastases in metavert-treated liver tissues (Fig. 5G). We noticed no-significant difference between the two conditions when staining with Sirius red suggesting no difference in fibrosis (Fig. 5H). Interestingly, staining of total and pro-cancer tumor associated macrophages (M2-like macrophages) showed a significant decrease of about 50% in the level of the pro-cancer tumor associated macrophages with metavert treatment as shown by the F4/80 and Arginase 1 staining (Fig. 5I). Measurement of cytokines associated with the inflammatory response and or stellate cell activation in mouse blood collected at the time of death of the mice showed a decrease in most of the pro-cancer cytokines measured. The most significant decreases were observed in cytokines IL-5, IL-1a, IL-18, and the chemokine, CCL5 (aka Lix). Other important pro-cancer cytokines and growth factors that were decreased in mice treated with metavert included IL-6, IL-4, IL-10, IL-22 and VEGF, among others (Fig. 6). Thus, the results indicated a decrease in the plasma level of pro-cancer cytokines involved in tumor promotion. The regulation of most of these cytokine productions has been shown to be mediated by transcription factors such as STAT3 and NF-κB in different cell types[45-50]. Our data shows that metavert, indeed, decreases the phosphorylation/activation levels of STAT3 and p65 of NF-κB in pancreatic cancer cells (Fig. S3A). Differently, and as it's expected from the inhibition of GSK3B, metavert induced an increase in the protein level of β-catenin (Fig. S3B).

Metavert treatment induced increase in histone acetylation and in phosphorylation/inhibition at Serine 9 of GSK3B (Fig. S4A) in the pancreas of KPC mice consistent with specificity shown by biophysical and *in vitro* studies. Treatment with metavert did not show noticeable toxicity; we did not observe any change in the behavior, food intake or activity of the mice between the 2 groups. The weight of mice was similar between the 2 groups (Fig. S4B). Measurements of markers of damage of liver and kidneys showed no significant difference between control and metavert-treated mice (Fig. S4C).

In a different experiment, KPC mice were treated with Gemcitabine alone or in combination with metavert. Metavert significantly improved the median survival time of KPC mice from 145 (Gemcitabine alone) to 230 days when treated with a combination of Gemcitabine and metavert (Fig. 5J) confirming the *in vitro* data showing sensitization of cancer cells to chemotherapies by metavert.

It's worth noting that a set of KPC mice (6 mice per group at the age of 2 months) were treated with vehicle or metavert for 2 months and then sacrificed. We found that the pancreas in control group was markedly enlarged and stretched in the abdomen compared to metavert-treated mice where the pancreas was still in its normal position without enlargement (Fig. S4D). The pancreas of the control group shows clear tumors occupying most of the pancreas space compared to smaller tumors and the presence of more normal-looking tissue in metavert-treated KPC mice as validated by H&E staining (Fig. S4E) and S100P staining (Fig. S4F). This data indicates that a short treatment with metavert decreases tumor growth.

To confirm the *in vivo* data in KPC mice we used a syngeneic model of PDAC by injecting the B6.129 mixed background mouse with mouse pancreatic cancer cells UN-KPC961-Luc expressing luciferase in the pancreas[51]. In the first set of mice (N=6) we treated mice for up

to 2 months after surgery to determine the survival curve. Imaging of the tumors after 3 weeks of treatment showed a decrease in tumor size in mice treated with metavert compared to control-treated mice (Fig. S5A). The survival data shows a significant increase in survival from a median survival of 86 days to 115 days (Fig. S5B). In a separate set of experiment, 4 mice per group were treated with and without metavert for 4 weeks and then sacrificed. Pancreatic size showed significant decrease in metavert-treated mice compared to control group (60% decrease) (Fig. S5C). Liver observation showed presence of tumors in 2/4 of control mice compared to none in treated mice (Fig. S5D). This data was similar to what we observed in the first set of syngeneic mice where 2/6 mice showed presence of liver metastasis compared to none in the liver of metavert-treated mice. Of note, one of the 4 metavert-treated mice died before the sacrificing time due an injury during injections.

Metavert effects on metabolic profile of cancer cells.

Recent studies show that HDAC and GSK3B increase glucose metabolism and induce cell proliferation in liver cancer and basal-like breast cancer cells, respectively[52, 53]. There are, however, no such evidence in PDAC cells. In this regard, we analyzed the effect of metavert on glucose metabolism using ^{13}C-glucose and mass spectroscopy[27]. We found that metavert decreased glucose oxidation in the TCA cycle as measured by ^{13}C-labeled CO2 production (Fig. 7A). In addition, the treatment increased the accumulation of glycogen (Fig. 7B). Because of these effects, metavert caused a decrease of nucleic acid ribose backbone synthesis (Fig. 7C) and decreased lactate formation from ^{13}C-glucose (Fig. 7D). Measurement of mitochondrial function showed increased ROS production associated with an increase in the total number of mitochondria per cell (Fig. 7E, F) suggesting shifting the phenotype of the cancer cell toward a normal cell -like phenotype.

The Scheme in the figure S6 represents how metavert regulates glucose metabolism in the cancer cells shifting the metabolic phenotype of the cancer cells toward a more normal-like phenotype by decreasing glucose utilization needed for proliferation, increasing the number of mitochondria, and forcing cells to alternative energy sources (possibly fatty acids). These findings reveal that metavert re-establishes the altered metabolic pathways often referred to as the Warburg effect of increased glycolysis and lactic acid formation in cancer cells.

DISCUSSION:

Our study aimed at designing and testing the effects of blocking both HDAC and GSK3B by a new chemical entity, metavert. Our data confirms the binding of metavert to both targets. The *in vitro* data showed an additive effect when combining HDAC-I/II and GSK3B inhibitors on preventing cancer cell survival. This effect was further associated with inhibition of the EMT pathway. It's worth noting that the intended effect of the HDAC inhibitor or metavert is through the classes I and II of HDAC but not classes III (sirtuins) and IV.

Our biophysical studies demonstrate that metavert binds to its targets with micromolar affinity. Although the affinity is in the micromolar scale, the disassociation rate (k_{off}) is in the order of 10^{-3} to 10^{-4} which suggest a longer residence time which induces the expected inhibitory effects. Metavert demonstrated improved biological effects on cancer cell survival

compared to the combination of specific inhibitors of HDAC and GSK3B. Used alone, the anti-cancer effects (as measured by IC50) of metavert were achieved at doses as low as 300nM to 1μM depending on cell lines and had no effect on the normal cells suggesting that the agent has low toxicity at the effective doses tested. Furthermore, metavert reduced cancer cell migration as measured by Matrigel cell invasion assay at 150nM and completely prevented the migration at 600nM which associated with a decrease in the expression of EMT and cancer stemness markers. The effect of metavert on EMT, migration and cancer stemness is more potent than the effect observed on cancer cell survival per se. Unexpectedly, metavert also affected metabolic profiles of tumor cells. Metavert decreased complete glucose oxidation in the TCA cycle suggesting that it promotes alternate fatty acid substrate oxidation in mitochondria. In fact, glucose uptake was increased by metavert; however, the glucose metabolism was decreased most likely because of the use of glucose for glycogen synthesis instead of producing substrates for building blocks for proliferation and use in the TCA cycle. This effect is most-likely induced by the inhibition of GSK3B by metavert, which then activates glycogen synthase and therefore shifts the fate of glucose from ribose synthesis and TCA cycle metabolism to glycogen synthesis. These findings reveal the possibility that overexpression of GSK3B in many cancers is responsible for the altered metabolic pathways often referred to as the Warburg effect of increased glycolysis and increased lactate produced from glucose metabolism, often associated with mitochondrial dysfunction. Metavert was observed to increase the number of mitochondria per cell and reverses the Warburg effect outcomes.

The potency of these effects suggest that it may have a particularly beneficial role when used with other potent chemotherapeutic agents known to enhance EMT and cancer stemness[54, 55]. Although systematically untested, it's worth noting that the combination of metavert with radiotherapy or a low dose of chemotherapy drugs gemcitabine and paclitaxel induced an additive or synergistic effect on PDAC survival. Our *in vivo* data showed a strong anti-cancer effect of metavert as it significantly increased the median survival time of KPC mice from 120 to 173 days. Most importantly, metavert completely prevented metastasis in these mice. The data was further confirmed using a syngeneic mouse model of pancreatic cancer. The importance of this data comes from the fact that most chemotherapy drugs used for treating PDAC increase the rate of metastasis and cancer stemness[54, 55]. Metavert is expected to reverse this side effects when combined with these chemotherapies. Indeed, we found that metavert increased the KPC mice survival time by 50% when added to gemcitabine compared to gemcitabine treatment alone.

Metavert altered not only tumor cell features, but also its microenvironment. Metavert treatment resulted in a marked decrease in circulating concentrations of multiple pro-cancer cytokines. One important cytokine is IL-6, which we have shown before to mediate interaction between cancer cells and macrophages involving a change in macrophage phenotype towards the pro-cancer tumor associated macrophage phenotype[17]. In fact, one of the striking features of the KPC mice treated with metavert was the decrease in pro-cancer tumor associated M2 macrophages by more than 50%. Of note, total number of macrophages did not change significantly. These results suggest regulation of the immune response by metavert by favoring the phenotype change of macrophages from the pro-cancer M2-like phenotype to the anti-cancer M1 phenotype. In addition to IL-6, other results we

have reported before suggest that a decrease in IL-4 and IL-13 also contributed to the regulation of macrophages phenotype[56]. Both cytokines were decreased by metavert in the blood of KPC mice. The effect of metavert on collagen production (a marker of fibrosis) and stellate cell activation showed no significant difference between the two groups indicating that most likely metavert has little effect on the pro-fibrotic function of stellate cells. In fact, the role of stellate cells in the pancreatic tumor microenvironment is debatable as studies show both a pro-cancer and anti-cancer role of these cells[57,58].

In sum, we have developed, synthesized and tested a novel molecule, metavert, that simultaneously inhibits two enzymes highly active in PDAC. We found metavert significantly reduced tumor size, prevented metastasis, and significantly extended survival of mice with the most aggressive form of PDAC. Metavert shifts the phenotype of the cancer cells towards a more normal-like phenotype and promotes anti-tumor effects synergistically with current modes of therapy. Metavert displays beneficial effect by affecting epithelial, metabolic and immunological response, which was unexpected, but could prove to be a unique drug in the field of cancer therapy. Finally, we demonstrated that metavert is a potent tool in the treatment of PDAC and possibly other cancers.

Supplementary Material

Refer to Web version on PubMed Central for supplementary material.

Acknowledgments:

We thank Dr. Yoshiko Machida and Dr. Makoto Kamata for generating the KPC mice and Dr. M-S Tsao for providing HPDE6-c7 cells.

This work was supported by the NIAAA grant K01 AA019996 and the Hirshberg Foundation Award (to ME), the NCI grant P01CA163200, the NIAAA grant P50AA011999, the Department of Veterans Affairs (to SJP), and the Samuel Oschin Comprehensive Cancer Institute Developmental Funds for Liver Metastasis Team Grant Research Award *"Colon, pancreas, and prostate cancer engraftment in the liver metastatic niche"*. And the Luke Wu-Jei Chang Discovery Fund.

REFERENCES:

1. Arora S, Bhardwaj A, Singh S, et al. An undesired effect of chemotherapy: gemcitabine promotes pancreatic cancer cell invasiveness through reactive oxygen species-dependent, nuclear factor kappaB- and hypoxia-inducible factor 1alpha-mediated up-regulation of CXCR4. J Biol Chem 2013;288:21197–207. [PubMed: 23740244]
2. Ryan Q, Ibrahim A, Cohen MH, et al. FDA drug approval summary: lapatinib in combination with capecitabine for previously treated metastatic breast cancer that overexpresses HER-2. Oncologist 2008;13:1114–9. [PubMed: 18849320]
3. Kanwal R, Gupta S. Epigenetic modifications in cancer. Clin Genet 2012;81:303–11. [PubMed: 22082348]
4. Kockeritz L, Doble B, Patel S, et al. Glycogen synthase kinase-3--an overview of an over-achieving protein kinase. Curr Drug Targets 2006;7:1377–88. [PubMed: 17100578]
5. Mamaghani S, Patel S, Hedley DW. Glycogen synthase kinase-3 inhibition disrupts nuclear factor-kappaB activity in pancreatic cancer, but fails to sensitize to gemcitabine chemotherapy. BMC Cancer 2009;9:132. [PubMed: 19405981]
6. Ougolkov AV, Fernandez-Zapico ME, Savoy DN, et al. Glycogen synthase kinase-3beta participates in nuclear factor kappaB-mediated gene transcription and cell survival in pancreatic cancer cells. Cancer Res 2005;65:2076–81. [PubMed: 15781615]

7. Ougolkov AV, Fernandez-Zapico ME, Bilim VN, et al. Aberrant nuclear accumulation of glycogen synthase kinase-3beta in human pancreatic cancer: association with kinase activity and tumor dedifferentiation. Clin Cancer Res 2006;12:5074–81. [PubMed: 16951223]
8. Ye Y, Xiao Y, Wang W, et al. ERalpha signaling through slug regulates E-cadherin and EMT. Oncogene 2010;29:1451–62. [PubMed: 20101232]
9. Zhou B, Gao WY, Zhang TJ, et al. [Study on the preparation and quality standard of Ephedra sinica dispensing granules]. Zhong Yao Cai 2006;29:1236–8. [PubMed: 17228668]
10. Thiery JP. Epithelial-mesenchymal transitions in development and pathologies. Curr Opin Cell Biol 2003;15:740–6. [PubMed: 14644200]
11. Tsuji T, Ibaragi S, Hu GF. Epithelial-mesenchymal transition and cell cooperativity in metastasis. Cancer Res 2009;69:7135–9. [PubMed: 19738043]
12. Aghdassi A, Sendler M, Guenther A, et al. Recruitment of histone deacetylases HDAC1 and HDAC2 by the transcriptional repressor ZEB1 downregulates E-cadherin expression in pancreatic cancer. Gut 2012;61:439–48. [PubMed: 22147512]
13. Kurahara H, Takao S, Maemura K, et al. Epithelial-mesenchymal transition and mesenchymal-epithelial transition via regulation of ZEB-1 and ZEB-2 expression in pancreatic cancer. J Surg Oncol 2012;105:655–61. [PubMed: 22213144]
14. Bachelder RE, Yoon SO, Franci C, et al. Glycogen synthase kinase-3 is an endogenous inhibitor of Snail transcription: implications for the epithelial-mesenchymal transition. J Cell Biol 2005;168:29–33. [PubMed: 15631989]
15. Zheng H, Li W, Wang Y, et al. Glycogen synthase kinase-3 beta regulates Snail and beta-catenin expression during Fas-induced epithelial-mesenchymal transition in gastrointestinal cancer. Eur J Cancer 2013;49:2734–46. [PubMed: 23582741]
16. Hingorani SR, Petricoin EF, Maitra A, et al. Preinvasive and invasive ductal pancreatic cancer and its early detection in the mouse. Cancer Cell 2003;4:437–50. [PubMed: 14706336]
17. Edderkaoui M, Xu S, Chheda C, et al. HDAC3 mediates smoking-induced pancreatic cancer. Oncotarget 2016.
18. Hingorani SR, Wang L, Multani AS, et al. Trp53R172H and KrasG12D cooperate to promote chromosomal instability and widely metastatic pancreatic ductal adenocarcinoma in mice. Cancer Cell 2005;7:469–83. [PubMed: 15894267]
19. Furukawa T, Duguid WP, Rosenberg L, et al. Long-term culture and immortalization of epithelial cells from normal adult human pancreatic ducts transfected by the E6E7 gene of human papilloma virus 16. Am J Pathol 1996;148:1763–70. [PubMed: 8669463]
20. Ouyang H, Mou L, Luk C, et al. Immortal human pancreatic duct epithelial cell lines with near normal genotype and phenotype. Am J Pathol 2000;157:1623–31. [PubMed: 11073822]
21. Edderkaoui M, Lugea A, Hui H, et al. Ellagic acid and embelin affect key cellular components of pancreatic adenocarcinoma, cancer, and stellate cells. Nutr Cancer 2013;65:1232–44. [PubMed: 24127740]
22. Edderkaoui M, Hong P, Lee JK, et al. Insulin-like growth factor-I receptor mediates the prosurvival effect of fibronectin. J Biol Chem 2007;282:26646–55. [PubMed: 17627944]
23. Edderkaoui M, Hong P, Vaquero EC, et al. Extracellular matrix stimulates reactive oxygen species production and increases pancreatic cancer cell survival through 5-lipoxygenase and NADPH oxidase. Am J Physiol Gastrointest Liver Physiol 2005;289:G1137–47. [PubMed: 16037546]
24. Lee JK, Edderkaoui M, Truong P, et al. NADPH oxidase promotes pancreatic cancer cell survival via inhibiting JAK2 dephosphorylation by tyrosine phosphatases. Gastroenterology 2007;133:1637–48. [PubMed: 17983808]
25. Suhane S, Kanzaki H, Arumugaswami V, et al. Mitochondrial NDUFS3 regulates the ROS-mediated onset of metabolic switch in transformed cells. Biol Open 2013;2:295–305. [PubMed: 23519235]
26. Xu Q, Biener-Ramanujan E, Yang W, et al. Targeting metabolic plasticity in breast cancer cells via mitochondrial complex I modulation. Breast Cancer Res Treat 2015;150:43–56. [PubMed: 25677747]

27. Tedeschi PM, Markert EK, Gounder M, et al. Contribution of serine, folate and glycine metabolism to the ATP, NADPH and purine requirements of cancer cells. Cell Death Dis 2013;4:e877. [PubMed: 24157871]
28. Edderkaoui M, Xu S, Chheda C, et al. HDAC3 mediates smoking-induced pancreatic cancer. Oncotarget 2016;7:7747–60. [PubMed: 26745602]
29. Gertych A, Wawrowsky KA, Lindsley E, et al. Automated quantification of DNA demethylation effects in cells via 3D mapping of nuclear signatures and population homogeneity assessment. Cytometry A 2009;75:569–83. [PubMed: 19459215]
30. Oh JH, Gertych A, Tajbakhsh J. Nuclear DNA methylation and chromatin condensation phenotypes are distinct between normally proliferating/aging, rapidly growing/immortal, and senescent cells. Oncotarget 2013;4:474–93. [PubMed: 23562889]
31. Habtezion A, Kwan R, Akhtar E, et al. Panhematin provides a therapeutic benefit in experimental pancreatitis. Gut 2011;60:671–9. [PubMed: 21159893]
32. Morin A, Eisenbraun B, Key J, et al. Collaboration gets the most out of software. Elife 2013;2:e01456. [PubMed: 24040512]
33. Lauffer BE, Mintzer R, Fong R, et al. Histone deacetylase (HDAC) inhibitor kinetic rate constants correlate with cellular histone acetylation but not transcription and cell viability. J Biol Chem 2013;288:26926–43. [PubMed: 23897821]
34. Friesner RA, Murphy RB, Repasky MP, et al. Extra precision glide: docking and scoring incorporating a model of hydrophobic enclosure for protein-ligand complexes. J Med Chem 2006;49:6177–96. [PubMed: 17034125]
35. Ouaissi M, Silvy F, Loncle C, et al. Further characterization of HDAC and SIRT gene expression patterns in pancreatic cancer and their relation to disease outcome. PLoS One 2014;9:e108520. [PubMed: 25275504]
36. Kitano A, Shimasaki T, Chikano Y, et al. Aberrant glycogen synthase kinase 3beta is involved in pancreatic cancer cell invasion and resistance to therapy. PLoS One 2013;8:e55289. [PubMed: 23408967]
37. Mann BS, Johnson JR, Cohen MH, et al. FDA approval summary: vorinostat for treatment of advanced primary cutaneous T-cell lymphoma. Oncologist 2007;12:1247–52. [PubMed: 17962618]
38. Lovestone S, Boada M, Dubois B, et al. A phase II trial of tideglusib in Alzheimer's disease. J Alzheimers Dis 2015;45:75–88. [PubMed: 25537011]
39. Monzon JG, Dancey J. Combination Agents versus Multi-Targeted Agents-Pros and Cons Cambridge, UK: Royal Society Cambridge, 2012.
40. Finnin MS, Donigian JR, Cohen A, et al. Structures of a histone deacetylase homologue bound to the TSA and SAHA inhibitors. Nature 1999;401:188–193. [PubMed: 10490031]
41. Dominguez JM, Fuertes A, Orozco L, et al. Evidence for irreversible inhibition of glycogen synthase kinase-3beta by tideglusib. J Biol Chem 2012;287:893–904. [PubMed: 22102280]
42. Castro A, Encinas A, Gil C, et al. Non-ATP competitive glycogen synthase kinase 3beta (GSK-3beta) inhibitors: study of structural requirements for thiadiazolidinone derivatives. Bioorg Med Chem 2008;16:495–510. [PubMed: 17919914]
43. Park BW, Zhang HT, Wu C, et al. Rationally designed anti-HER2/neu peptide mimetic disables P185HER2/neu tyrosine kinases in vitro and in vivo. Nat Biotechnol 2000;18:194–8. [PubMed: 10657127]
44. Zapata M, Cohen C, Siddiqui MT. Immunohistochemical expression of SMAD4, CK19, and CA19–9 in fine needle aspiration samples of pancreatic adenocarcinoma: Utility and potential role. Cytojournal 2007;4:13. [PubMed: 17587453]
45. Kim JY, Bae YH, Bae MK, et al. Visfatin through STAT3 activation enhances IL-6 expression that promotes endothelial angiogenesis. Biochim Biophys Acta 2009;1793:1759–67. [PubMed: 19751774]
46. Stritesky GL, Muthukrishnan R, Sehra S, et al. The transcription factor STAT3 is required for T helper 2 cell development. Immunity 2011;34:39–49. [PubMed: 21215659]
47. Libermann TA, Baltimore D. Activation of interleukin-6 gene expression through the NF-kappa B transcription factor. Mol Cell Biol 1990;10:2327–34. [PubMed: 2183031]

48. Mori N, Prager D. Transactivation of the interleukin-1alpha promoter by human T-cell leukemia virus type I and type II Tax proteins. Blood 1996;87:3410–7. [PubMed: 8605359]

49. Smith JB, Wadleigh DJ, Xia YR, et al. Cloning and genomic localization of the murine LPS-induced CXC chemokine (LIX) gene, Scyb5. Immunogenetics 2002;54:599–603. [PubMed: 12439624]

50. Kortylewski M, Xin H, Kujawski M, et al. Regulation of the IL-23 and IL-12 balance by Stat3 signaling in the tumor microenvironment. Cancer Cell 2009;15:114–23. [PubMed: 19185846]

51. Torres MP, Rachagani S, Souchek JJ, et al. Novel pancreatic cancer cell lines derived from genetically engineered mouse models of spontaneous pancreatic adenocarcinoma: applications in diagnosis and therapy. PLoS One 2013;8:e80580. [PubMed: 24278292]

52. Yang J, Jin X, Yan Y, et al. Inhibiting histone deacetylases suppresses glucose metabolism and hepatocellular carcinoma growth by restoring FBP1 expression. Sci Rep 2017;7:43864. [PubMed: 28262837]

53. Gupta C, Kaur J, Tikoo K. Regulation of MDA-MB-231 cell proliferation by GSK-3beta involves epigenetic modifications under high glucose conditions. Exp Cell Res 2014;324:75–83. [PubMed: 24704462]

54. Volk-Draper L, Hall K, Griggs C, et al. Paclitaxel therapy promotes breast cancer metastasis in a TLR4-dependent manner. Cancer Res 2014;74:5421–34. [PubMed: 25274031]

55. Zhang Z, Duan Q, Zhao H, et al. Gemcitabine treatment promotes pancreatic cancer stemness through the Nox/ROS/NF-kappaB/STAT3 signaling cascade. Cancer Lett 2016;382:53–63. [PubMed: 27576197]

56. Xue J, Sharma V, Hsieh MH, et al. Alternatively activated macrophages promote pancreatic fibrosis in chronic pancreatitis. Nat Commun 2015;6:7158. [PubMed: 25981357]

57. Ozdemir BC, Pentcheva-Hoang T, Carstens JL, et al. Depletion of carcinoma-associated fibroblasts and fibrosis induces immunosuppression and accelerates pancreas cancer with reduced survival. Cancer Cell 2014;25:719–34. [PubMed: 24856586]

58. Wilson JS, Pirola RC, Apte MV. Stars and stripes in pancreatic cancer: role of stellate cells and stroma in cancer progression. Front Physiol 2014;5:52. [PubMed: 24592240]

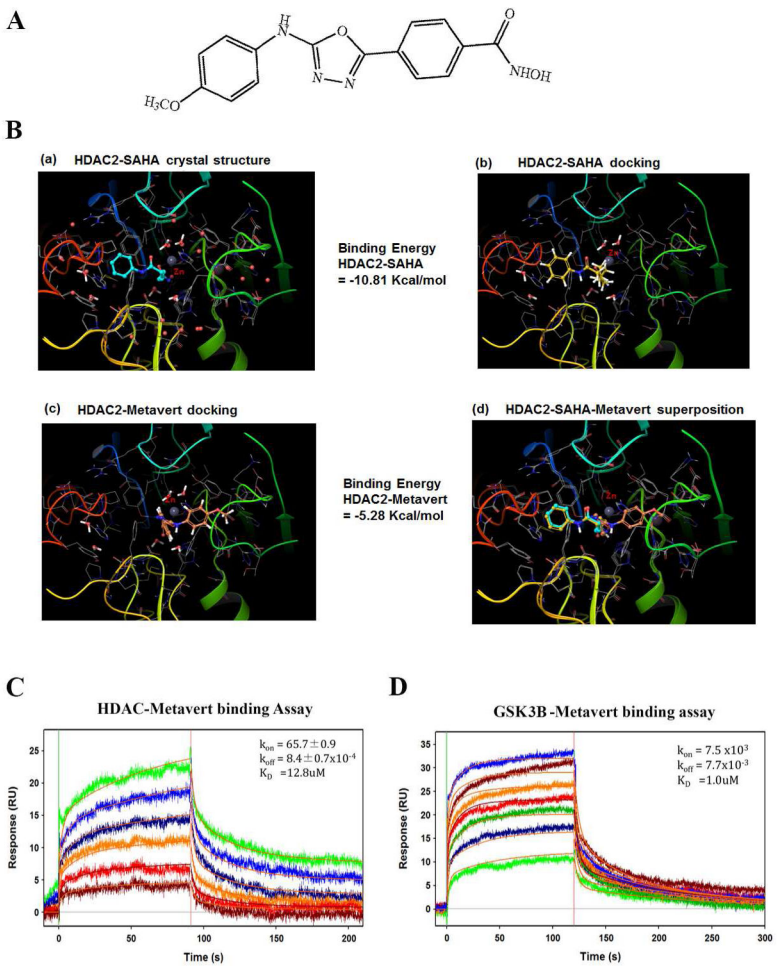

Figure 1: Molecular models and binding studies of HDAC2/ GSK3B with metavert.

(A) Structure of metavert. (B) Molecular models of metavert and Saha binding to HDAC2. (B-a) Binding of Saha in the crystal structure of HDAC2. Zinc (Zn): gray sphere. (B-b) Binding mode of Saha using docking procedure reproduces the binding mode observed in the crystal structure. (B-c) Binding mode of metavert in HDAC2. (B-d) Superposition of Saha and metavert binding to HDAC2. (C, D) Binding analysis using surface plasmon resonance (SPR). Metavert was analyzed at serial doubling concentrations maximized at 100 μM. (C) Highest concentration in green and lowest in brown for HDAC2 binding, and (D) in Blue and green, respectively, for GSK3B binding.

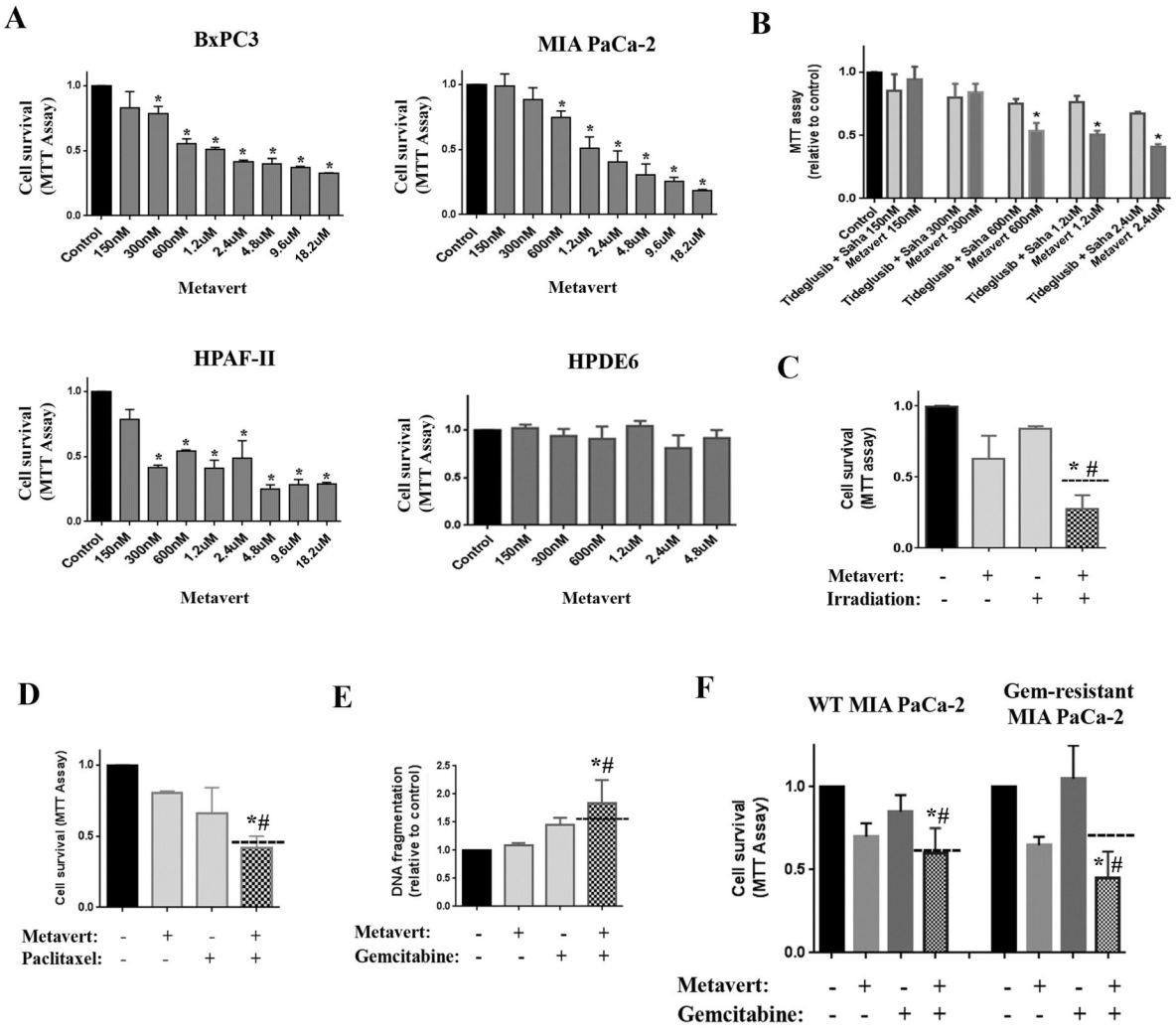

Figure 2: Metavert significantly decreases pancreatic cancer cell survival and sensitizes cells to treatments without affecting normal cells.

MIA PaCa-2 (A-B, D-F), BxPC-3 (A, C), HPAF-II (B) and HPDE6 (B) cells were cultured for 72h with different doses of metavert. (A-D, F) Cell survival was measured by MTT assay. (E) Apoptosis was measured by assessing DNA fragmentation. (B) Cells were cultured in the presence of a combination of indicated doses of metavert or Tideglusib and Saha. (D) BxPC-3 cells were cultured with 2.4μM metavert for 24h, then exposed to 4Gy irradiation and cultured for another 72h. MIA PaCa-2 cells cultured with Gemcitabine (Gem) 1ng/ml and metavert (150nM) (E) or 600nM (F) for 72h. *, $p < 0.05$ *versus* control; #, $p < 0.05$ *versus* the same dose of the combination of Tideglusib and Saha (B) or *versus* irradiation or chemotherapy treatment (C-F). Dashed lanes represent the expected additive effect.

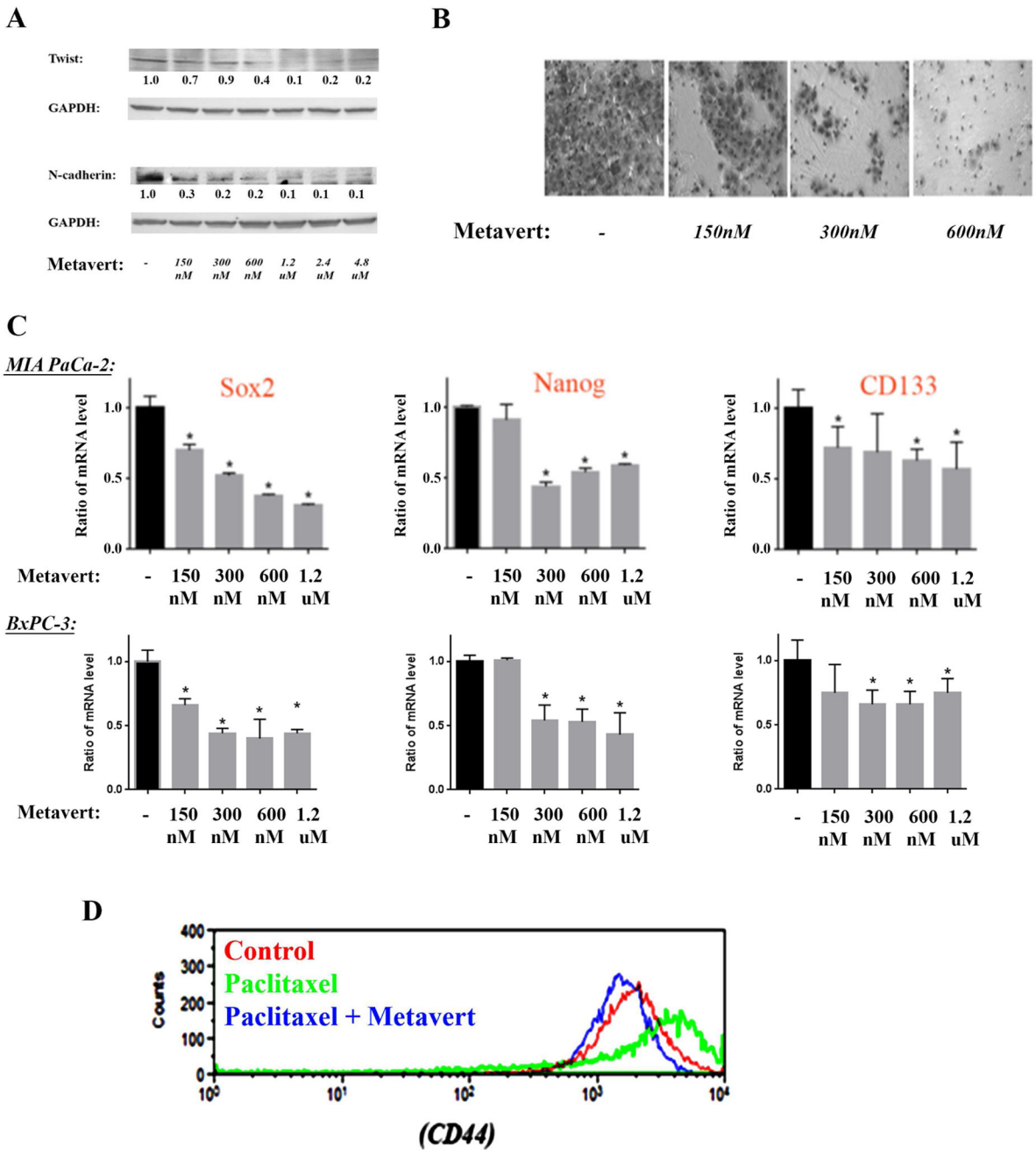

Figure 3: Metavert prevents migration, EMT and cancer stemness markers in cancer cells.

MIA PaCa-2 and BxPC-3 cells were cultured for 72h with different doses of metavert. (A) Protein levels in MIA PaCa-2 were measured by Western. Blots were re-probed for GAPDH to confirm equal loading. (B) MIA PaCa-2 cell migration was measured by Matrigel Invasion Assay. After 72h treatment, 100,000 cells were re-plated overnight for the invasion assay. The total number of cells did not change during the overnight invasion assay. (C) mRNA levels were measured by RT-PCR in MIA PaCa-2 and BxPC-3 cells. (D) Level of

CD44 was measured by flow cytometry using CD44 (PE/Cy7) antibody in MIA PaCa-2 cells treated with metavert (600nM) or Paclitaxel (10nM).

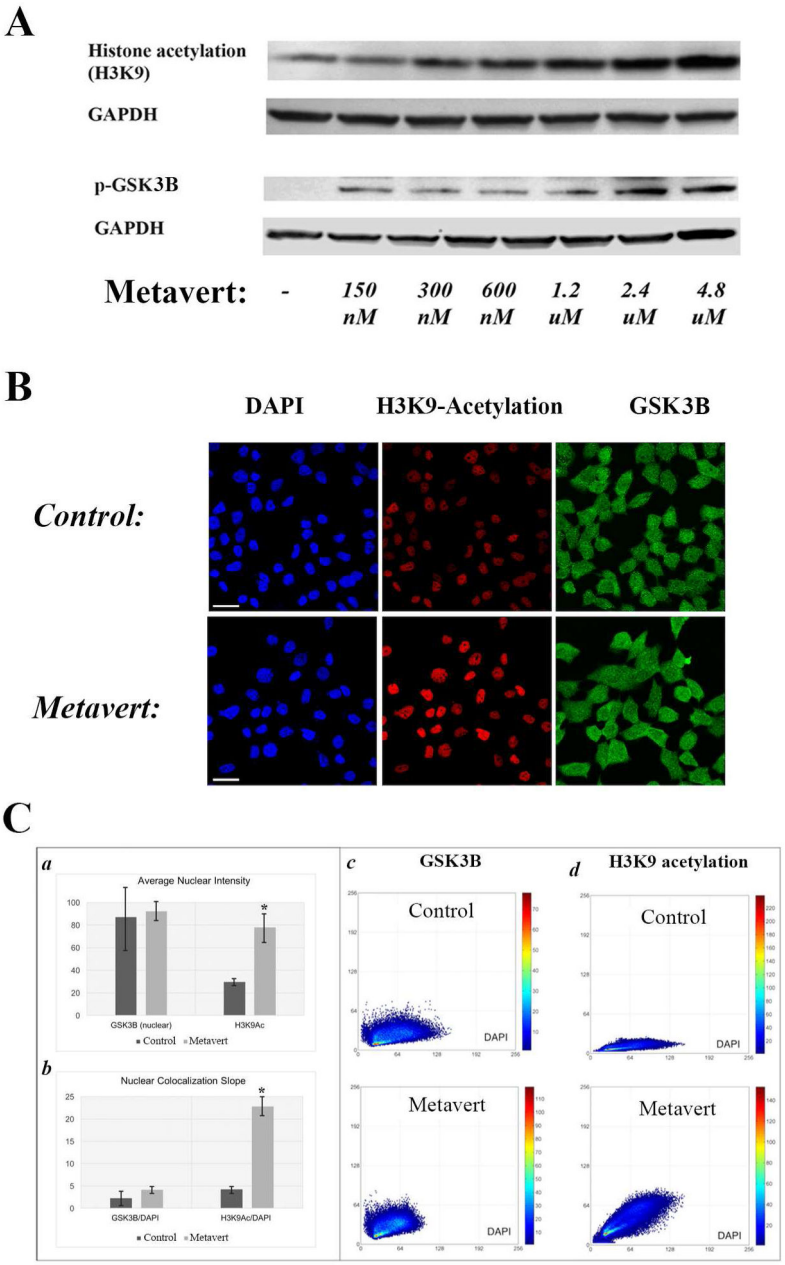

Figure 4: Effect of metavert on its expected targets.

MIA PaCa-2 cells were cultured for 72h with metavert (1.2μM) or indicated doses. (A) levels of proteins were measured by Western. Membranes were re-probed for GAPDH to confirm equal loading. (B) Maximum intensity projections of confocal images of cells that were immunofluorescent co-labeled for GSK3B (green) and H3K9Ac (red) and counterstained with DAPI (blue). (C) Quantitative results of cell-by-cell high-content analysis of untreated control cells versus metavert-treated cells: Average nuclear intensities (a) and average values for slopes of the co-localization scatter plots (b) of GSK3B and H3K9Ac across all analyzed cells are displayed as bar plots. Representative scatter plots of

single cells for GSK3B /DAPI (c) and H3K9 acetylation/DAPI (d). *, $p < 0.05$ *versus* control.

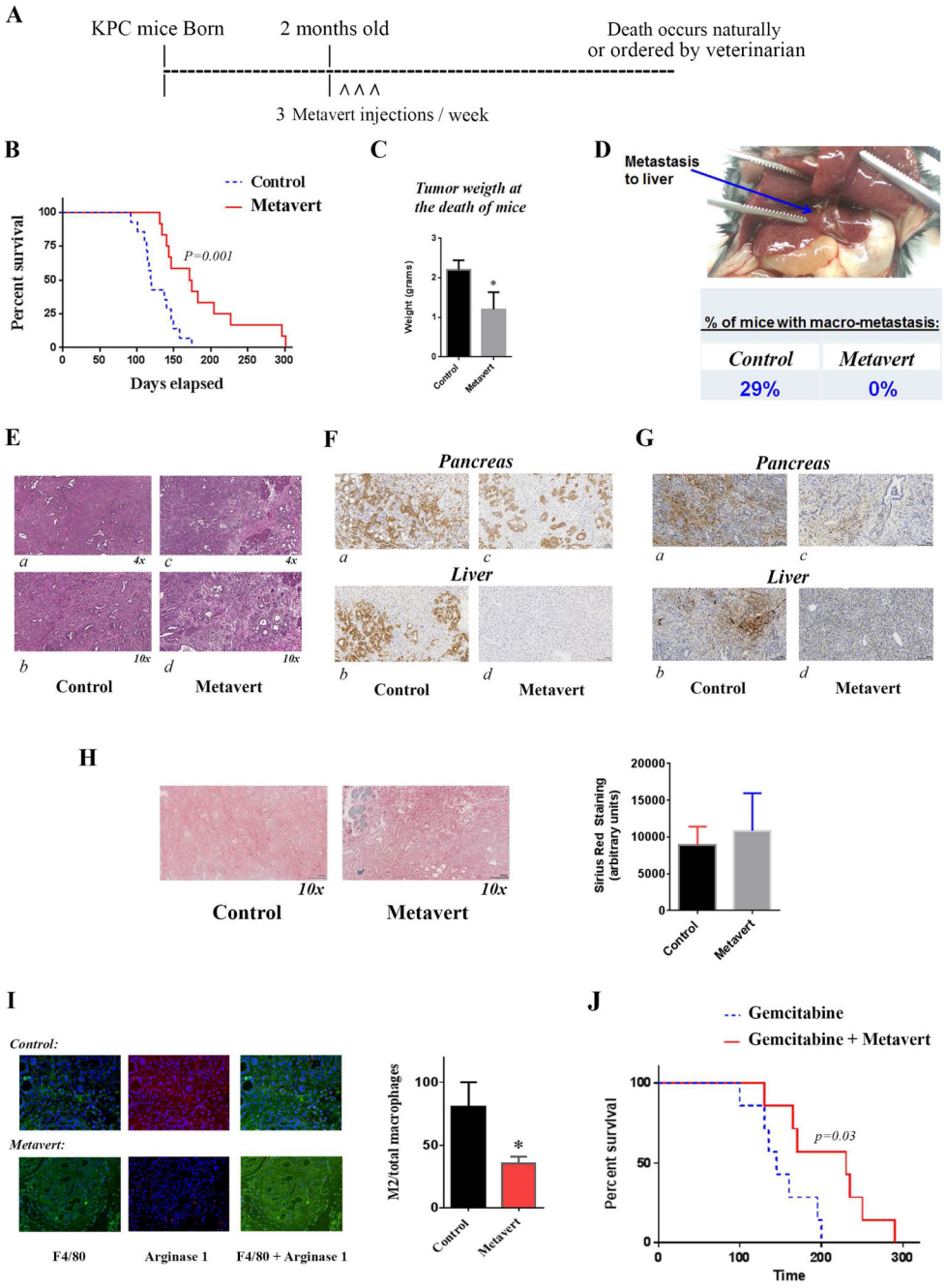

Figure 5: Metavert significantly increases survival of KPC mice and completely prevents metastasis.

KPC mice were intraperitoneally injected starting from the age of 2 months with 5mg/Kg of metavert 3 times per week (A). (B) Survival data of KPC mice. (C) Tumor weight at the death of mice. (D) Liver metastasis and quantification of percentage of mice with metastasis. (E) H&E staining of pancreatic tissue from control mice (a, b) and metavert-treated mice (c, d). (F) CK19 staining of pancreatic and liver tissues from control mice (a, b) and metavert-treated mice (c, d). (G) S100P staining of pancreatic and liver tissues from control mice (a, b) and metavert-treated mice (c, d). (H) Sirius Red/Collagen staining of KPC mice pancreas

with quantification. (I) M2 macrophage staining with F4/80 and Arginase1 antibodies and quantification. (J) Survival data of KPC mice intraperitoneally injected with Gemcitabine (10mg/Kg) once a week and metavert (5mg/Kg) 3 times per week. *, $p < 0.05$ *versus* control.

	Control (pg/ml)	Metavert (pg/ml)	*p* Value
IL-6	158.20	51.44	0.02
IL-5	31.96	11.11	0.04
IL-1a	44.93	14.80	0.03
Lix	66.78	34.53	0.04
IL-18	491.10	234.20	0.01
IL-4	71.86	22.39	0.07
IL-1b	4.98	0.64	0.06
IL-10	29.72	4.66	0.07
IL-17A	12.22	2.59	0.08
IL12-P70	1.61	0.40	0.12
IL-31	12.05	5.40	0.13
MIP-1b	9.16	1.79	0.14
IL-13	92.29	33.62	0.16
IL-22	66.49	17.32	0.17
IL-23	38.29	7.10	0.19
MIP-1a	20.87	3.34	0.21
TGF-b	74.91	15.42	0.22
IFN-g	2.61	0.71	0.22
LIF	28.80	9.20	0.28
VEGF	10.47	5.92	0.28

Figure 6: Cytokine levels in the plasma of KPC mice.

Cytokines in the blood collected from KPC mice at the time of death were measured using multiplexing ELISA.

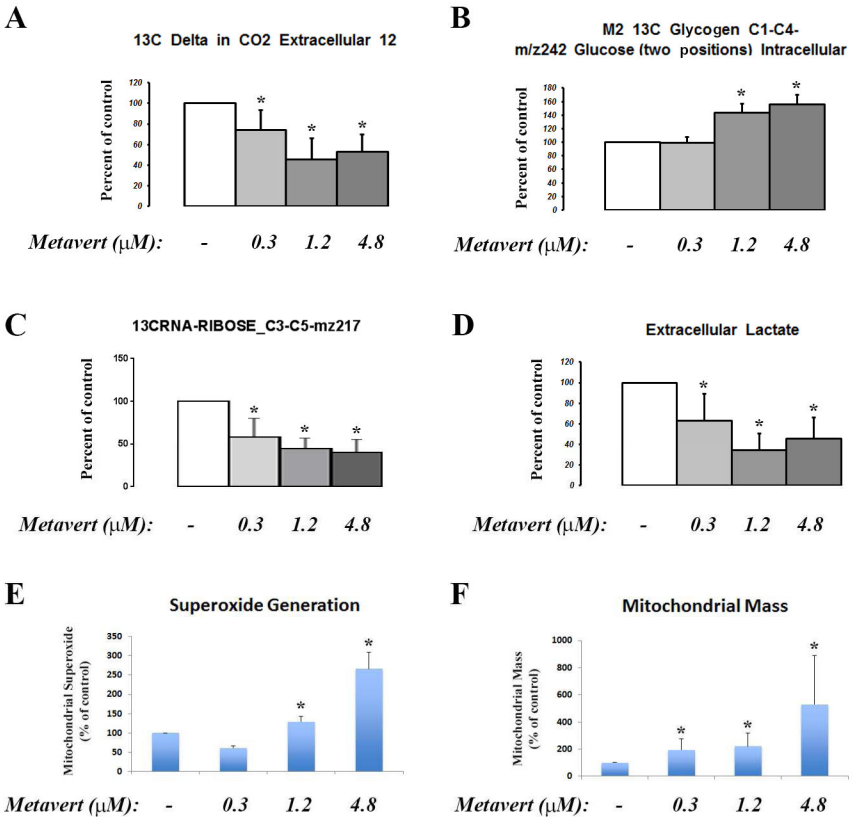

Figure 7: Metavert affects glucose metabolism in cancer cells.

BxPC-3 cancer cells were cultured with ^{13}C-glucose and treated with indicated doses of metavert for 72h. (A-D) Mass spectroscopy of indicated ^{13}C-labeled products. (A) Level of CO2, (B) Intracellular glycogen level, (C) ribose, and (D) extracellular lactic acid. (E) Level of superoxide production measured by MitoSox Red labeling. (F) Mitochondrial mass measured using mitotracker green probe and flow cytometry. *, $p < 0.05$ *versus* control.